Published online 18 May 2016

Nucleic Acids Research, 2016, Vol. 44, No. 15 ***7251–7266***
doi: 10.1093/nar/gkw449

Role of the Polymerase ϵ sub-unit DPB2 in DNA replication, cell cycle regulation and DNA damage response in Arabidopsis

José Antonio Pedroza-Garcia[1,2], Séverine Domenichini[1,2], Christelle Mazubert[1,2], Mickael Bourge[3], Charles White[4], Elodie Hudik[1,2], Rémi Bounon[1,2], Zakia Tariq[1,2], Etienne Delannoy[1,2], Ivan del Olmo[5], Manuel Piñeiro[5], Jose Antonio Jarillo[5], Catherine Bergounioux[1,2], Moussa Benhamed[1,2] and Cécile Raynaud[1,2,*]

[1]Institute of Plant Sciences Paris Saclay IPS2, CNRS, INRA, Université Paris-Sud, Université Evry, Université Paris-Saclay, Bâtiment 630, 91405 Orsay, France, [2]Institute of Plant Sciences Paris-Saclay IPS2, Paris Diderot, Sorbonne Paris-Cité, Bâtiment 630, 91405 Orsay, France, [3]Institute of Integrative Biology of the Cell (I2BC), CEA, CNRS, Univ. Paris-Sud, Université Paris-Saclay, 91198 Gif-sur-Yvette, France, [4]Génétique, Reproduction et Développement, UMR CNRS 6293/Clermont Université/INSERM U1103, 63000 Clermont-Ferrand, France and [5]CBGP (INIA-UPM) Departamento de Biotecnología, Instituto Nacional de Investigación y Tecnología Agraria y Alimentaria, Campus de Montegancedo, Madrid 28223, Spain

Received February 12, 2016; Revised May 07, 2016; Accepted May 09, 2016

ABSTRACT

Faithful DNA replication maintains genome stability in dividing cells and from one generation to the next. This is particularly important in plants because the whole plant body and reproductive cells originate from meristematic cells that retain their proliferative capacity throughout the life cycle of the organism. DNA replication involves large sets of proteins whose activity is strictly regulated, and is tightly linked to the DNA damage response to detect and respond to replication errors or defects. Central to this interconnection is the replicative polymerase DNA Polymerase ϵ (Pol ϵ) which participates in DNA replication *per se*, as well as replication stress response in animals and in yeast. Surprisingly, its function has to date been little explored in plants, and notably its relationship with DNA Damage Response (DDR) has not been investigated. Here, we have studied the role of the largest regulatory sub-unit of Arabidopsis DNA Pol ϵ: DPB2, using an over-expression strategy. We demonstrate that excess accumulation of the protein impairs DNA replication and causes endogenous DNA stress. Furthermore, we show that Pol ϵ dysfunction has contrasting outcomes in vegetative and reproductive cells and leads to the activation of distinct DDR pathways in the two cell types.

INTRODUCTION

In all living organisms, DNA replication is the fundamental process that faithfully duplicates the genome prior to its distribution between daughter cells during cell division. Plants continuously form new organs throughout their life cycle thanks to meristematic cells that retain their proliferative capacity and also give rise to reproductive cells relatively late in the life of the plant. One mechanism that has been proposed to avoid extensive accumulation of replication errors in meristems is the presence of slowly dividing cells in its centre that divide less frequently than their neighbours, and can thus function as a reservoir of cells in which genome integrity is preserved (1). However, it is also possible that plant-specific mechanisms exist to avoid the accumulation of errors during DNA replication.

In both prokaryotes and eukaryotes, the DNA replication machinery is a complex and dynamic structure called the replisome. The eukaryotic replisome comprises an 11 subunit helicase complex and replicative DNA polymerases (2). The helicase activity is brought by the MCM2-7 (Mini Chromosome Maintenance) heterohexamer that forms a ring unwinding unreplicated DNA. To be activated, the MCM complex needs to associate with the GINS (consisting of four proteins (Sld5-Psf1-Psf2-Psf3) named for

*To whom correspondence should be addressed. Tel: +33 1 69 15 33 98; Email: cecile.raynaud@u-psud.fr
Present addresses:
Elodie Hudik, Université Paris-Sud, Orsay F-91405, France; CNRS U8000, LCP, Orsay F-91405, France.
Rémi Bounon, INRA, US1279 Etude du Polymorphisme des Génomes Végétaux, CEA-IG/Centre National de Génotypage EVRY 91057, France.

the Japanese 'go-ichi-ni-san', which means 5-1-2-3) and CDC45. All together these sub-units form the CMG complex (CDC45, MCM, GINS). Once the replication fork is opened by the CMG, chromosomes are replicated by the DNA polymerase α/primase complex that synthesizes primers for the leading strand and Okazaki fragments, and Polymerases δ and ϵ that are thought to elongate these primers (2), but whose respective roles at the fork are debated. For the past few years, the generally accepted view has been that Pol δ synthesizes the lagging strand (3) while Pol ϵ is responsible for the synthesis of the leading strand (4). However, recent work suggests that polymerase δ replicates both strands, while Pol ϵ would be involved in the removal of replication errors generated by Pol δ (5), and would play an important scaffolding role at the fork.

Although it may not be responsible for DNA synthesis *per se*, DNA Pol ϵ is of particular interest because it stands at the interface between DNA replication, DNA repair, cell cycle regulation upon DNA damage and chromatin remodelling (6). In yeast and animals, it is a four sub-unit complex comprising a catalytic sub-unit (Pol2A) and three accessory sub-units DPB2, 3 and 4 (6), that are not required for the DNA polymerase activity. The largest accessory sub-unit, DPB2, is essential to cell viability and could be involved in the stabilization of the Pol ϵ complex (6). In addition, DPB2 interacts with Psf1, thereby inserting Pol ϵ in the replisome on the leading strand (7,8). Another unique feature of Pol ϵ is its involvement in DNA stress response: yeast mutants in the C-terminal region of its catalytic sub-unit are sensitive to Hydroxy-Urea (HU) induced replication stress and undergo catastrophic mitosis, indicating that they fail to activate the appropriate checkpoint (9). This function appears to be conserved in animals (6), but the underlying molecular mechanisms remain unclear. In addition, replication stress has been shown to induce degradation of DNA Pol ϵ, which could thus function both as a sensor and a target of DNA Damage Response (DDR) (10).

DDR has been studied into detail in yeast and animals. Briefly, two main protein kinases ATM (Ataxia Telangiectasia Mutated) and ATR (ATM and Rad3 related) are involved respectively in the perception of double-strand breaks and single stranded DNA. Once activated, they trigger a phosphorylation cascade leading to the activation of p53, a transcription factor which in turn stimulates the expression of DNA repair genes, checkpoint factors that delay cell cycle progression etc. (11). Because fork stalling can lead to the dissociation of the helicase complex from the polymerases and thus formation of large stretches of single stranded DNA, ATR is the main kinase involved in replication stress response (11). Its activation at replication forks involves the detection of single-stranded DNA coated with the RPA protein on the leading strand and activation by the 9-1-1 complex on the lagging strand (11). Interestingly, Puddu *et al.* have reported that the yeast ATR homolog Mec1 can be activated by replication stress via two independent pathways, one of which requires the C-terminus of Pol2A as well as the accessory sub-unit DPB4 (12). Mechanisms involved in DNA replication and DDR appear to be conserved in plants, but are poorly described compared to animal or yeast models.

All components of the replisome and DNA polymerases are conserved in plants (13). The Arabidopsis genome encodes two isoforms of the catalytic sub-unit (Pol2A and Pol2B), one DPB2 sub-unit (14) (At5g22110), two putative homologues of DPB3 and one DPB4 (15). Genetic analysis revealed that the *emb529* or *tilted1* mutants lacking Pol2A or *cyclops2* (*cyl2*) lacking DPB2 are arrested at very early stage during embryo development, which precluded detailed analysis of the Pol ϵ function or of its interaction with DNA damage response (14,16). However, identification of Pol2A, Pol2B and DPB2 as sub-units of DNA polymerase is corroborated by their expression in dividing tissues, as well as by the observation that treatment with the replication inhibitor aphidicolin induces similar embryo development defects as the ones observed in *Pol2A* or *DPB2* deficient mutants, and that DPB2 interacts with the C-terminus of Pol2A (14,16). By contrast, evidence for a role of putative DPB3 or DPB4 homologues in DNA replication is lacking, and the Arabidopsis DPB3-1 protein appears to participate in the transcriptional regulation of heat-stress genes (17). More recently, the isolation of hypomorphic alleles of Pol2A has shed more light on the biological function of Pol ϵ in plants. Both *abo4* (*abscisic acid over-sensitive*) and *esd7* (*early in short days*) mutants display partial loss of function of Pol2A and show reduced growth, as well as disorganized meristems and early flowering (18,19), providing evidence for the role of Pol ϵ in the replication of the genetic and epigenetic information (20). In addition, *abo4* mutants show enhanced recombination and expression of DNA repair genes, indicating that the role of Pol ϵ in the perception of DNA stress during S-phase may be conserved in plants (18).

The main actors of the DNA damage response and S-phase checkpoint are also conserved in plants, although many intermediaries of the phosphorylation cascade are apparently missing (21). The Arabidopsis genome encodes one ATM and one ATR kinase; mutants deficient for these proteins are viable although double mutants are completely sterile (22). Like in other eukaryotes, ATM appears to be predominantly involved in double-strand break perception whereas ATR senses replication stress and induces G2 cell cycle arrest after DNA damage (22,23). Both ATM and ATR can activate the SOG1 transcription factor, the functional homologue of p53, which in turn stimulates the expression of DNA repair genes (24). Activation of ATM or ATR by DNA damage also causes programmed induction of endoreduplication (several rounds of DNA replication without mitosis, (25)), cell cycle arrest via activation of the WEE1 protein kinase which inhibit CDK (Cyclin Dependent Kinase)/Cyclin complexes (26) and in some instances programmed cell death (27). The plant DDR and more specifically the replication stress response is thus beginning to be well described (28). Nevertheless, the relationships between DNA replication proteins such as Pol ϵ and DDR remain to be fully elucidated. In addition, very little is known regarding the contribution of accessory sub-units to this interconnection since null mutants are lethal and no partial loss of function mutant has been isolated.

In this work, we have generated over-expression lines to gain insight into the role of the largest accessory sub-unit of Pol ϵ DPB2 and its genetic interaction with DDR pathways.

MATERIALS AND METHODS

Cloning procedures

DPB2 cDNA was amplified using the DPB2 EcoRI and DPB2 XhoI stop primers and clones between the EcoRI and XhoI sites of the pENTR^{TM}3C vector (Life Technologies). To generate the DPB2-CFP construct, the cDNA was subsequently transferred to the pB7CWG2 vector (https://gateway.psb.ugent.be/search) using the Gateway technology according to manufacturer's instructions. To generate a DPB2 over-expression construct without adding a tag to the protein, the cDNA was recombined in the pK7WG2 vector (https://gateway.psb.ugent.be/search). For *cyl2* mutant complementation, the 35S promoter of the pH7FWG2 (https://gateway.psb.ugent.be/search) was replaced by the *DPB2* promoter described in (14) amplified with primers introducing a HindIII and a SpeI site at its 5′ and 3′ ends respectively. The *DPB2* cDNA alone or the *CFP-DPB2* cDNA was subsequently cloned downstream of the *DPB2* promoter. To generate DPB2-RNAi inducible lines, a 500bp fragment of the DPB2 cDNA was cloned between the EcoRI and KpnI and ClaI and BamHI sites of the pKannibal vector. The RNAi cassette was then transferred to a modified pPZP111 downstream of the *alcA* promoter for inducible expression as described in (29). Sequence for primers is provided in Supplementary Table S1.

Plant material and growth conditions

Seeds were surface-sterilized by treatment with bayrochlore for 20 min, washed and imbibed in sterile-water for 2–4 days at 4°C to obtain homogeneous germination. Seeds were sown on commercially available 0.5× Murashige and Skoog (MS) medium (Basalt Salt Mixure M0221, Duchefa) with the appropriate antibiotic if needed and solidified with 0.8% agar (Phyto-Agar HP696, Kalys), and grown in a long days (16 h light, 8 h night, 21°C) growth chamber. After 2 weeks, the plants were transferred to soil in a glasshouse under short-day conditions (8 h light 20°C, 16 h night at 18°C) for 2 weeks before being transferred to long-day conditions. For selection of *DBP2OE* lines, seeds of the T1 generation were sown on sand and watered with a solution of glufosinate (7.5 mg/l). Independent lines were allowed to self-fertilize, and homozygous lines of the T3 generation were used for all subsequent experiments, unless otherwise specified.

RNA Extraction and quantitative RT-PCR

Total RNA were extracted from seedlings with the RNeasy MiniPrep kit (Qiagen, according to the manufacturer's instructions. First strand cDNA was synthesized from 2μg of total RNA using Improm-II reverse transcriptase (A3802, Promega) according to the manufacturer's instructions. 1/25th of the synthesized cDNA was mixed with 100nM of each primer and LightCycler® 480 Sybr Green I master mix (Roche Applied Science) for quantitative PCR analysis. Products were amplified and fluorescent signals acquired with a LightCycler® 480 detection system. The specificity of amplification products was determined by melting curves. *PDF2* was used as internal control for signals normalization. Exor4 relative quantification software (Roche Applied Science) automatically calculates relative expression level of the selected genes with algorithms based on ΔΔCt method. Data were from triplicates and are representative of at least two biological replicates. The sequence of primers used in this study is provided in Supplementary Table S1.

Transcriptome studies

Three independent biological replicates were produced. For each biological repetition and each point, RNA samples were obtained by pooling RNAs from more than 200 plants. Whole plantlets were collected on plants at 1.04 developmental growth stages (30), cultivated *in vitro* under long-day conditions. Total RNA was extracted as described above. RNA-seq experiment was carried out at the POPS Transcriptomic Platform, Institute of Plant Sciences - Paris-Saclay (Orsay, France). PolyA RNA was purified using the Dynabeads mRNA direct micro kit (Ambion, France). The sequencing libraries were constructed with the Ion Total RNA-Seq Kit v2 and the sequencing spheres were prepared with the Ion PI^{TM} Template OT2 200 Kit v3 before sequencing on an Ion Proton using the Ion PI^{TM} Sequencing 200 Kit v3 and Ion PI v2 chips (Life Technologies, France) with 520 run flows.

RNA-seq bioinformatic treatment and analysis

To allow comparisons, each RNA-Seq sample followed the same pipeline from trimming to count of transcript abundance as follows. Read preprocessing criteria included trimming library adapters and performing quality control checks using the Torrent suite (Version 4.2.1) with default settings. The reads corresponding to rRNAs were identified by mapping on *A. thaliana* rRNAs using bowtie version2 (with –local option) (31) and removed. The same software was used to align the remaining reads against the *A. thaliana* transcriptome (33 602 mRNA from TAIR 10 (32)) without ambiguous hits (multi-hits are removed). According to these rules, around 75% of the initial reads aligned to transcripts for each sample. Genes which do not have at least 1 read after a counts-per-million (CPM) normalization in at least three samples among the six were discarded. The differential analysis has been performed by using a likelihood ratio test in a negative binomial generalized linear model where the dispersion is estimated by the method proposed in edgeR and where a biological replicate effect was taken into account. A gene was declared differentially expressed if its raw *P*-value adjusted by the Benjamini-Hochberg procedure to control the FDR is <0.05. Analyses were performed with the software 'R' (Version 3.1.0) and the edgeR package (version 3.6.8) of Bioconductor.

Light and fluorescence microscopy

Fresh siliques were opened under a stereo-microscope (SVII, ZEISS) and images were captured with a colour CCD camera (Power HAD, Sony).

For meiotic analyses, flower buds were fixed in EtOH:acetic acid (3 :1). 4′,6-Diamidino-2-phenylindole staining of meiotic chromosomes was performed according to a previously described method (33). Slides were observed

on an epi-fluorescence videomicroscope (SVII; Zeiss), and images were captured with a colour charge-coupled device camera (Power HAD; Sony).

For cell cycle length analysis, we used a method adapted from (34). Plants were grown on supplemented MS medium (10 g l^{-1} sucrose, 0.1 g l^{-1} myo-inositol, 0.5 g l^{-1} MES, 100 μl thiamine hydrochloride (10 mg ml^{-1}), 100 μl pyridoxine (5 mg ml^{-1}), 100 μl nicotinic acid (5 mg ml^{-1}), pH 5.7, adjusted with 1 m KOH, and 10 g l^{-1} agar) for 5 days, and transferred to the same medium supplemented with EdU (10 μM). Samples were collected after 3, 6, 9 and 12 h, fixed in paraformaldehyde (4% in PME buffer:50 mm piperazine-*N*,*N*′-bis(2-ethanesulphonic acid) (PIPES), pH 6.9; 5 mM $MgSO_4$; 1 mM EGTA) for 45 min and washed with PME buffer. Root apices were dissected on a glass slide and digested in a drop of enzyme mix (1% (w/v) cellulase, 0.5% (w/v) cytohelicase, 1% (w/v) pectolyase in PME) for 1h at 37°C. After three washes with PIPES, root apices were squashed gently between the slide and a coverslip, and frozen in liquid nitrogen. After removal of the coverslip and drying of the slides for 1h at room temperature, EdU revelation and Hoechst counterstaining were performed as described in (35). The percentage of EdU positive nuclei was plotted as a function of time. The percentage of EdU positive nuclei increases linearly with time, and follows an equation that can be written as $P = at + b$ where y is the percentage of EdU positive nuclei and t is time. Total cell cycle length is estimated as $100/a$, and S phase length is b/a.

Detection of γ-H2AX foci by immunostaining was performed as described previously (36).

Flow cytometry

For flow cytometric nuclei analysis, tissues were chopped with a razor blade in 1 ml of Gif nuclei-isolation buffer (45 mM $MgCl_2$, 30 mM sodium citrate, 60 mM MOPS, 1% (w/v) polyvinylpyrrolidone 10 000, pH 7.2) containing 0.1% (w/v) Triton X-100, supplemented with 5 mM sodium metabisulphite and RNAse (5 U/ml). Propidium iodide was added to the filtered supernatants to a final concentration of 50 μg/ml. Endoreduplication levels of 5000–10 000 stained nuclei were determined using a Cyflow SL3 flow cytometer (Partec-Sysmex) with a 532-nm solid state laser (30 mW) excitation and an emission collected after a 590-nm long-pass filter. For cell cycle analysis, we used the algorithm available in the Flomax software.

For EdU incorporation analysis, plantlets were incubated on MS supplemented with EdU (10 μM) for 7 h. Nuclei were extracted as described above, pelleted by centrifugation (5 min at 1000 g). The revelation reaction was performed as described in (35) and analysed on a Moflo Astrios flow cytometer (Beckman-Coulter).

Histochemical staining of GUS activity

After 15-min fixation in 100% cold acetone, β-glucuronidase (GUS) activity was revealed as described previously (37). After 1 h at 37°C, samples were washed in 70% ethanol, fixed with PFA during 20 min under vacuum, and then cleared using chloral hydrate solution overnight at room temperature (8 g of chloral hydrate (Sigma), 2 ml of 50% glycerol and 1 ml of water). Images were captured on a macroscope (AZ100, NIKON) with a video camera Nikon RI1.

Statistical analysis

All statistical analysis was performed using the R software (https://www.r-project.org/).

RESULTS

Molecular and morphological characterization of the DPB2 over-expressing lines

Dpb2 null mutants are lethal (14), and partial loss-of-function lines are not available. To decipher the biological function of DPB2, we thus generated lines over-expressing the DPB2 protein fused to CFP under the control of a 35S promoter (hereafter referred to as *DPB2OE*). In the T1 generation, *DPB2OE* plants displayed severe developmental defects including reduced stature and partial or complete sterility depending on the severity of the phenotype (Figure 1A). Three independent over-expresser lines were selected for further analysis, and all subsequent experiments were performed on seeds of the T3 generation. These lines were selected because they were representative of the different classes of phenotype observed, *DPB2OE 1* being the most, and *DPB2OE 3* the less severely affected (Figure 1B). The degree of phenotypic alterations during development correlated with *DPB2* transcript accumulation (Figure 1C). In addition to reduced rosette size and stem height, root growth was inhibited in these lines, similarly to that observed in the *abo4-1* mutant which is deficient for the catalytic sub-unit of Pol ϵ ((18), Figure 1D). As shown on Supplementary Figure S1A and B, the CFP-DPB2 fusion expressed downstream of the *DPB2* promoter could complement the *cyl2* mutant which is deficient for DPB2 (14), indicating that the tagged version of DPB2 is functional. Identical phenotypes were observed in lines over-expressing DPB2 without tag (Supplementary Figure S1C), further confirming that the observed defects are due to excess accumulation of a functional DPB2 protein.

Plants displaying the most severe phenotype (*DPB2OE1*, Figure 1A) in the T1 generation displayed reduced fertility, and some were completely sterile. The latter lines displayed few pollen grains of very heterogeneous size, which prompted us to analyse meiosis progression in wild-type (Figure 2A–E) and these *DPB2OE* lines (Figure 2F–I). In the wild-type chromosomes condense during prophase I to form bivalents (Figure 2A and B). Homologous chromosomes segregate during the first division (Figure 2C), and sister chromatids segregate during the second (Figure 2D) to form tetrads (Figure 2E). Although the early steps of meiosis appeared normal in *DPB2OE* (Figure 2F), bivalents were never identified. Instead, we observed severe chromosome fragmentation both during the first and the second meiotic division (Figure 2G-H) resulting in the formation of polyads (Figure 2I) that contained unequal amounts of fragmented chromosomal material. During meiosis, the SPO11 endonuclease produces programmed double-strand breaks (DSB) to initiate homologous recombination, cross-over formation and thereby chromosome

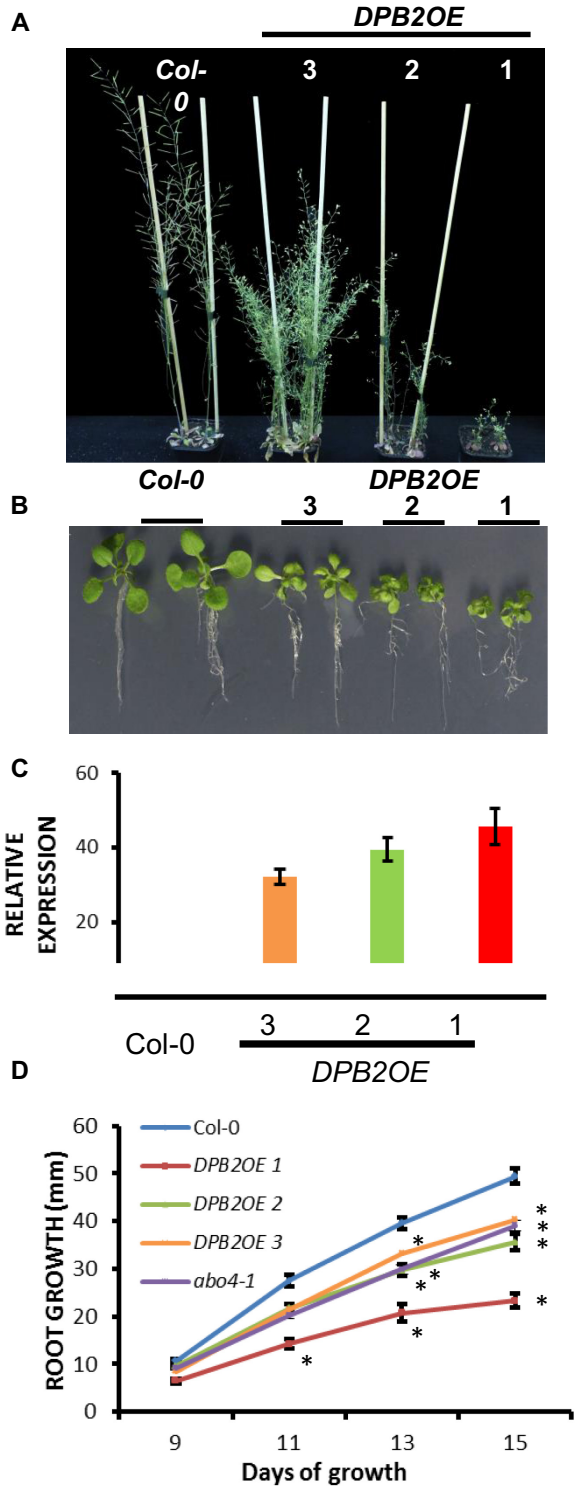

Figure 1. *DPB2* over-expression inhibits plant growth. (**A**) Six-week-old plants display severe dwarfism compared to the wild type. (**B**) Seedlings of 14 days-old of wild-type (Col-0) and three independent *DPB2OE* lines. (**C**) Quantification of *DPB2* expression in the wild-type (Col-0) and three independent *DPB2OE* lines by RT-qPCR. Results are average standard deviation (SD) from three technical replicates and are representative of two independent experiments. (**D**) Root growth is reduced in *DPB2OE* lines. Wild-type (Col0) and *DPB2OE* lines were grown vertically for 2 weeks, and root length was measured every second day. The *abo4-1* mutant (18) that is deficient for the catalytic sub-unit of Pol e was included as a control. Growth reduction was similar in *abo4-1* and in *DPB2OE* 2 and *3*, but more pronounced in *DPB2OE1*. Error bars indicate the standard error (SE) between three biological replicates with 20 seedlings each. Asterisks indicate significant differences respect to wild type plants (Student's *t* test: $P < 0.05$).

pairing (38). To determine whether this fragmentation was due to defects in the repair of these DSB we introduced the *DPB2OE* construct in the *spo11-1* mutant (38). Because this mutant does not form DSB, homologous chromosomes do not pair and segregate randomly during the first meiotic division (Figure 2J), resulting in the formation of polyads containing random combinations of chromosomes (Figure 2L–M). Because Arabidopsis has few chromosomes, this abnormal meiosis does not result in complete sterility: one gamete in 32 is expected to contain exactly one chromosome of each pair. Chromosome fragmentation was identical in *spo11-1 DPB2OE* lines to that observed in *DPB2OE* lines with apparently normal early prophase (Figure 2N–Q). The failure of the *spo11-1* mutation to rescue *DPB2OE*-induced fragmentation was also reflected in the enhanced sterility of *spo11-1 DPB2OE* (Supplementary Figure S2), suggesting that DNA fragmentation occurred before SPO11 activation, possibly due to defects in pre-meiotic DNA replication.

DPB2 over-expression affects DNA replication and cell cycle progression

To evaluate whether the observed growth reduction of DPB2 over-expressing plants might be caused by defects in DNA replication, we first tested the sensitivity of *DPB2OE* lines to aphidicolin, an inhibitor of the B-family polymerases comprising the three replicative polymerases: α, δ and ϵ (39). We included the *abo4-1* mutant in this test as a control. Both genotypes were hyper-sensitive to aphidicolin compared to the wild-type: they displayed chlorotic leaves (Figure 3A and B) and reduction of root length (Figure 3C and D), indicating that *DPB2* over-expression, like the *abo4* mutation, impairs DNA replication. To corroborate this hypothesis, we generated ethanol-inducible RNAi lines targeting the *DPB2* transcript. Prolonged growth on ethanol resulted in complete growth arrest, but on low doses of ethanol plants could be maintained for a few days and, we observed a reduction of root elongation comparable to the one observed in *DPB2OE* lines (Supplementary Figure S3). Furthermore, plants over-expressing DPB2 showed a clear acceleration of flowering time as described for the Pol2A mutant *esd7*, providing further evidence for partial complex inactivation caused by excess DPB2 accumulation (Supplementary Figure S4).

To further analyse the DNA replication defects caused by *DPB2* over-expression, we monitored cell cycle progression in *DPB2OE* lines. We first performed flow cytometry analysis on cauline leaves of *DPB2OE* lines. Endoreduplication was increased in all *DPB2OE* lines (Figure 4A), regardless of the severity of the phenotype, indicating that *DPB2* over-expression induces extra rounds of DNA replication in developing organs. In addition, we reproducibly observed that flow-cytometry profiles obtained on lines displaying a se-

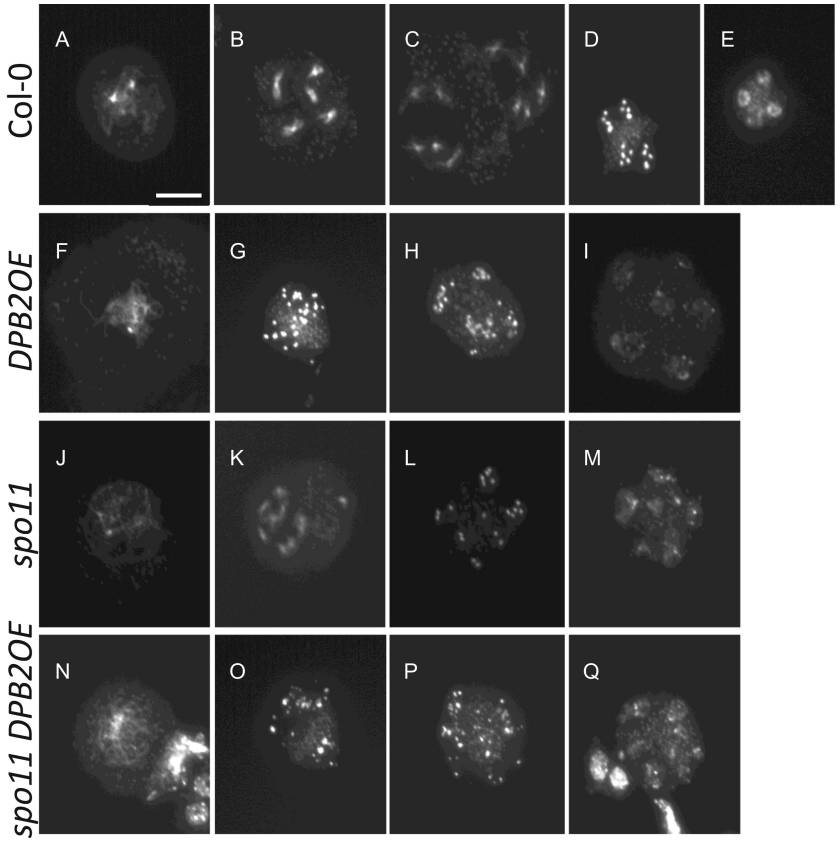

Figure 2. *DPB2* over-expression causes SPO11-independent DNA fragmentation during meiosis. Meiosis was observed in WT (**A**–**E**), *DPB2OE* (**F**–**I**), spo11 (**J**–**M**) and *spo11 DPB2OE* (**N**–**Q**) lines. In the wild-type, chromosomes begin to condense and pair during prophase I (**A**), until they form five bivalents displaying chiasmata (**B**). The first meiotic division segregates five homologue chromosome at each cellular pole (**C**), and sister chromatids segregate during the second meiotic division (**D**), resulting in the formation of tetrads (**E**). By contrast, in *DPB2OE*, although early steps of meiosis appeared normal (**F**), bivalents were never observed. Instead, severe chromosome fragmentation was observed both during the first (**G**) and the second meiotic division (**H**), resulting in the formation of polyads (**I**). In the *spo11* background, early steps of prophase I proceed normally (**J**), but chromosomes fail to pair due to the absence of double-strand breaks required to trigger the formation of crossing-overs. Instead, the first meiotic division randomly segregates 10 univalents (**K**). Subsequent segregation of sister chromatids during the second division (**L**) results in the formation of polyads (M), although a small number of balanced gametes are formed. Meiosis in *spo11 DPB2OE* lines was identical to that observed in *DPB2OE* lines with apparently normal early prophase (**N**), severe chromosome fragmentation visible both during D1 and D2 (**O**, **P**) and formation of polyads (**Q**). Bar in A = 10 μm for all panels.

vere phenotype showed poorly separated peaks compared to the wild-type (Figure 4B and C), suggesting that a higher proportion of nuclei contained intermediate DNA contents. To determine whether this phenomenon could be due to an increase in the proportion of S-phase nuclei, the cell cycle distribution of nuclei extracted from young flower buds was analysed. The proportion of S-phase cells was higher in *DPB2OE* lines, and the proportion of G1 cells was reduced (Figure 4D and E). This was reproducibly observed on independent samples (Figure 4F). To confirm that the proportion of nuclei in S-phase is increased in *DPB2OE* lines, we used ethynyl deoxyuridine (EdU) incorporation; EdU is a thymidine analogue that can be incorporated into genomic DNA during S-phase. The results obtained by EdU incorporation combined with flow-cytometry analysis of whole seedlings were consistent with an increased proportion of S-phase cells in *DPB2OE* lines (Figure 4G).

The observed increase in the proportion of S-phase cells could either be due to enhanced proliferative activity, or to a prolongation of S-phase duration. To discriminate between these two possibilities, we estimated cell cycle and S-phase length as described in (34) by following EdU incorporation as a function of time in root meristems of wild-type, *DPB2OE1* and *DPB2OE2* lines (Supplementary Figure S5). As shown in Table 1, total cell cycle length was increased in both *DPB2OE* lines. S-phase length was about twice that of the wild type for both lines. However, the increase of total cell cycle length was systematically higher than that of S-phase duration, indicating that another cell cycle phase (likely the G2 phase) was prolonged by *DPB2* over-expression. Furthermore, a similar increase in S-phase and cell cycle length was observed in *DPB2-RNAi* lines grown in the presence of ethanol for 3 days (Supplementary Figure S6), confirming that this increase in S-phase length is due to partial loss of Pol ϵ function.

In summary, these results suggest that *DPB2* over-expression affects cell cycle progression leading to an increase in S-phase length, possibly due to checkpoint activation.

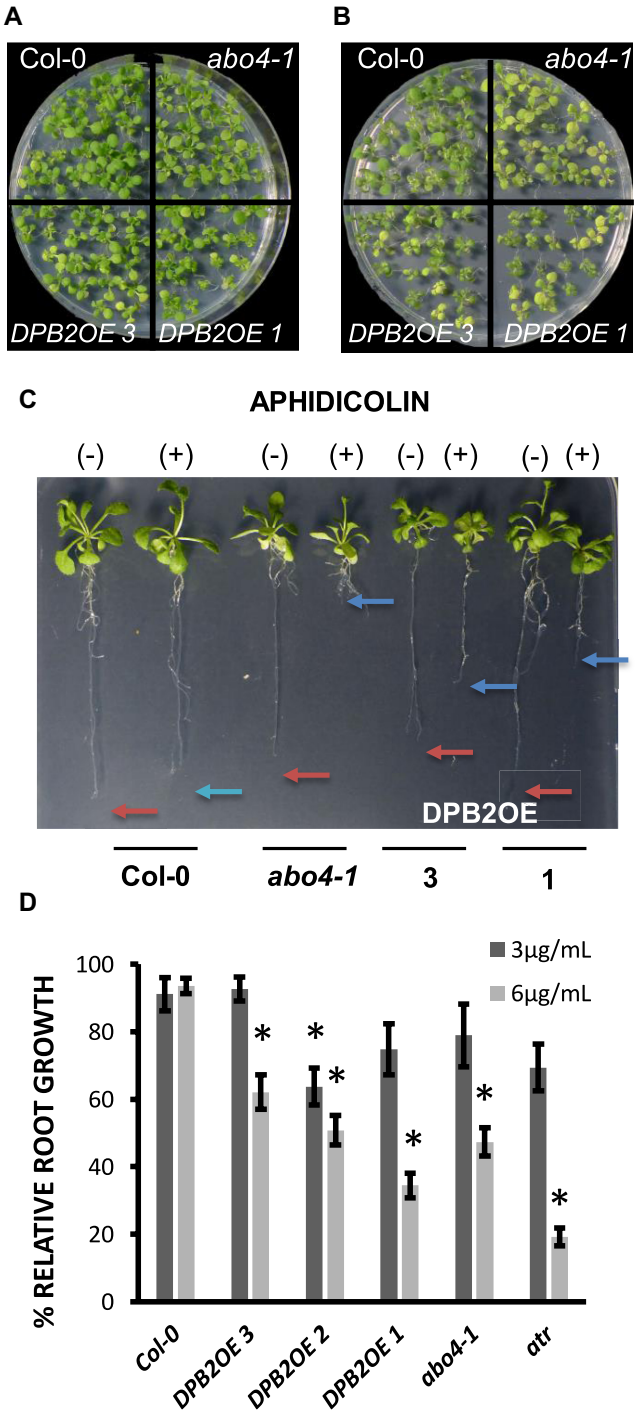

Figure 3. *DPB2OE* lines are hypersenstivite to the replication inhibitor aphidicolin. (A and B) Four-day-old seedlings of the wild-type (Col-0), *DPB2OE* and *abo4-1* mutants were transferred for 7 days to half-strength MS medium supplemented with aphidicolin 6 µg/ml (**B**) or DMSO (**A**). (**C**) Growth of seedlings after of 14 days on mock (DMSO) or aphidicolin 6 µg/ml. (**D**) Relative root growth of seedlings after a 14-day of growth on aphidicolin. The results are showed as the percentage with respect of the corresponding mock genotypes. Data represent mean ± SE of three independent experiments ($n = 25$ for each experiment), the asterisks denote significant difference with respect to wild type plants with the same treatment (Student's t test: $P < 0.05$).

Table 1. Cell cycle length is increased in *DPB2OE* lines

Line	Cell cycle length (h)		S-phase length (h)	
Col-0	19.5	20.4	3.7	3.3
DPB2OE1	26.3	27.2	7.4	7.3
DPB2OE2	24.4	23.3	6.7	6

Cell cycle and S-phase length were estimated as described in (34) by following EdU incorporation for 12h in root tip cells. Values are for two independent experiments.

DPB2 over-expression induces symptoms of DNA damage accumulation

To evaluate whether delay in the cell cycle progression observed in *DPB2OE* lines could be due to constitutive activation of the DDR, we analysed the presence of DNA damage hallmarks. Indeed, several mutants subjected to endogenous DNA stress show enhanced endoreduplication (28) which was the case in *DPB2OE* (Figure 4A). In addition, DNA stress often leads to increase expression of *CYCB1;1*. Consistently, in the absence of HU, the *CYCB1;1::DB-GUS DPB2OE* lines showed increased GUS staining in proliferating tissue compared to the wild-type (Supplementary Figure S7). This observation suggests that *DPB2* over-expression delays the G2/M progression possibly due to DNA damage stress. Furthermore, a number of genes that are upregulated in response to DNA damage such as *RAD51*, *CYCB1;1* or *PARP2* (23) were up-regulated in *DPB2OE* lines (Figure 5A).

To further investigate the effects of *DPB2* over-expression, the transcriptome of *DPB2OE* lines 1 and 3 was compared to that of wild-type plants by RNA sequencing. Overall 45 genes were significantly up-regulated in line 1, and 455 in line 3 whereas numbers of down-regulated genes were 319 and 640 respectively (fold change ≥ 1.5 P value ≤ 0.01; Supplementary Table S2). There was significant overlap between up-regulated genes in the two lines (Supplementary Figure S8A) and gene ontology analysis of significantly up-regulated genes in the two lines revealed over-representation of the 'DNA metabolic process' category (Supplementary Figure S8B). Consistently, among a set of 61 genes identified before as DNA stress hallmark genes (23,40), 28 were up-regulated in *DPB2OE* plants considering both RNA sequencings (Table 2). Although not all genes reported were up-regulated in both cases, RT-qPCR analysis revealed for example, that *RAD51* was up-regulated in all *DPB2OE* lines analysed (Figure 5A), and that failure to detect it as being mis-regulated in one of the lines was likely due to the heterogeneity of the replicates. To further corroborate that Pol ϵ dysfunction systematically results in activation of the DDR, expression of *PARP2*, *RAD51*, *XRI-1* and *BRCA1* was also monitored in *abo4-1* mutants and in inducible *DPB2-RNAi* lines (Figure 5B and C). As expected, all these genes were up-regulated in *abo4-1*, consistent with previous results (18). All five genes were also induced in both RNAi lines in the presence of ethanol, indicating that these lines have similar defects to *DPB2OE* plants.

To determine if the constitutive activation of DDR genes in *DPB2OE* lines was caused by accumulation of DNA damage, we performed *in situ* immuno-staining experiment

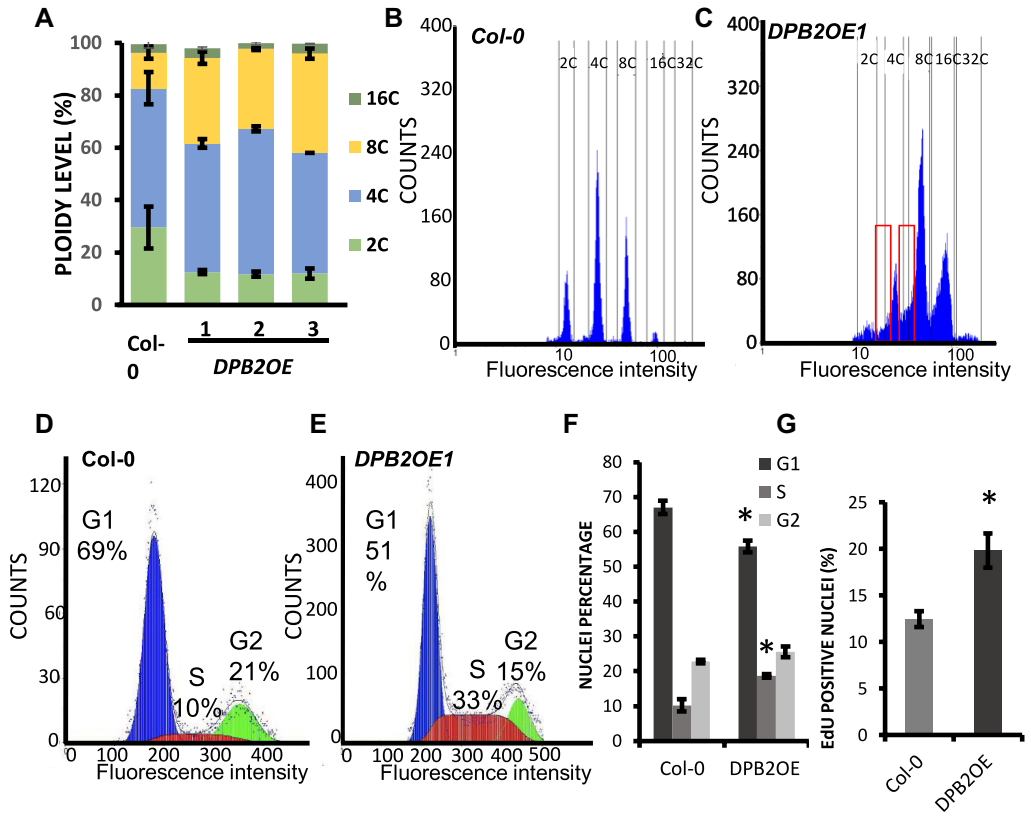

Figure 4. S-phase progression is impaired in *DPB2OE* plants. (**A**) Endoreduplication is increased in *DPB2OE* lines. The DNA content of nuclei extracted from the first cauline leaf of wild-type (Col-0) and three independent *DPB2OE* lines was analyzed by flow cytometry. All lines displayed an increased proportion of 8C nuclei and a decreased proportion of 2C nuclei, irrespective of the severity of the phenotype. Values are average ± SD ($n = 3$). (B and C) Flow-cytometry profiles obtained in Col-0 (**B**) and one *DPB2OE* line (**C**). The number of events (count) is plotted against fluorescence intensity (log scale). Peaks corresponding to different DNA contents are poorly separated in *DPB2OE* plants. Graph presented here are representative of more than 10 independent observations in three independent *DPB2OE* lines. (**D**–**F**) The proportion of S-phase nuclei is increased in *DPB2OE* lines. Nuclei were extracted from flower buds of the wild-type (Col-0) and *DPB2OE* lines, stained with propidium iodide and their DNA content was measured. A cell cycle was fitted on the profile, displaying G1 nuclei in blue, S nuclei in red and G2 nuclei in Green. The proportion of each type of nuclei is indicated in the graph (**D** and **E**), data are representative of 10 independent observations. (**F**) proportion of S-phase nuclei in flower buds of wild-type Col-0 and *DPB2OE* lines, data are average ± S.D. ($n = 3$ independent lines). (**G**) EdU incorporation is increased in *DPB2OE* lines. Seven-day-old plantlets were incubated for 3 h on 0.5× MS containing EdU, and the proportion of labelled nuclei was quantified by flow cytometry ($n = 10\,000$), the result is the average of three independent *DPB2OE* lines. For (F) and (G), the asterisks denote significant differences with respect to wild type plants (Student's t test; $P < 0.05$).

in *DPB2OE* root tip nuclei using γ-H2AX antibodies directed against the Arabidopsis protein (41,42). As expected, no foci were detected in root tips of wild type plants. In contrast *DPB2OE* roots displayed γ-H2AX foci (Figure 6). We observed ∼22% of nuclei containing at least one γ-H2AX focus in *DPB2OE 1* and 6% in *DPB2OE 2*. These results suggest that *DPB2OE* plants present endogenous DNA damage leading to constitutive activation of DDR.

Tolerance to DNA damage is increased in *DPB2OE* plants

The *abo4-1* mutant has been reported to be hypersensitive to DNA-damaging agents (18), indicating that the catalytic sub-unit of Pol ϵ is required for efficient DDR. To investigate the role of DPB2 in this process, we performed DNA damage sensitivity assays with *DPB2OE* seedlings. *atr* and *atm* mutants that are known to be sensitive to replicative stress and DSBs respectively were included as controls in our assays.

We first investigated the response to replication fork stalling. To this end, plants were exposed to different concentrations of hydroxyurea (HU), which is an inhibitor of ribonucleotide reductase. HU treatment depletes cellular deoxyribonucleotide pools, and thereby induces stalling of replication forks. The sensitivity to DNA stress was determined by assessing the proportion of plants displaying true leaves after 10 days of incubation on HU (43). This proportion was higher in all three *DPB2OE* lines than in the wild-type (Figure 7A and B), whereas the *atr* mutant showed increased sensitivity as expected. Because HU induces oxidative stress in the leaves (40), the effect of HU on root development was also monitored. Roots of *DPB2OE* displayed a lower growth-inhibition compared to the wild type (Figure 7C). Although the observed difference was relatively modest, it was statistically significant; suggesting that *DPB2OE* seedlings show increased tolerance to replication fork stalling. Since HU does not directly damage DNA, we also assessed the sensitivity of *DPB2OE* lines to a range of DNA-damaging agents. We used UV-C, the alkylating agents mitomycin C and methyl methanesulfonate (MMS) that produce both mutagenic and replication blocking le-

Table 2. DNA stress hallmark genes induced in *DPB2OE* seedlings compared with wild type

Locus	Description	*DPB2OE 1* Fold change	*DPB2OE3* Fold change
AT4G29170	Mnd1 family protein	2.3	2.6
AT3G27060	TSO2	1.9	2.5
AT4G02390	PARP-2	2.4	2.0
AT5G24280	Gamma-irradiation and mitomycin c induced 1	2.4	2.3
AT5G48720	X-ray induced transcript 1 (XRI1)	2.1	2.3
AT4G21070	Breast cancer susceptibility 1 (BRCA1)	2.8	3.3
AT2G30360	SOS3-interacting protein 4	2.2	2.3
AT5G61000	Replication protein a 1D (RPA1D)	1.9	1.8
AT4G19130	Replication protein A 1E (RPA1E)	2.0	2.3
AT5G23910	Kinesin-related, ComEA domain	2.1	1.8
AT2G21790	Ribonucleotide reductase 1 (RNR1)	1.7	1.7
AT3G07800	Thymidine kinase 1a (TK1a)	2.8	37
AT4G22960	Protein of unknown function (DUF544)	9.9	13.0
AT3G27630	Siamese-related 7 (SMR7)	5.0	9.9
AT5G60250	zinc finger (C3HC4-type RING finger) family protein	4.2	4.6
AT1G08260	Catalityc subunit of polymerase epsilon (POL2A)	1.8	–
AT5G03780	TRF-LIKE 10	2.4	–
AT1G20750	RAD3-LIKE	10.0	–
AT4G24610	unknown protein	1.8	–
AT5G55490	SMC1-related, SbcC-related, ZipA-related	6.4	–
AT5G20850	RAD51	–	2.5
AT4G25580	stress-responsive protein-related	–	3.6
AT5G64060	NAC domain containing protein 103	–	2.9
AT1G05490	Chromating remodeling 30	–	2.4
AT5G67460	O-Glycosyl hydrolases family 17 protein	–	2.0
AT3G45730	unknown protein	–	2.9
AT1G07500	Siamese-related 5 (SMR5)	–	17.3

- : no significant difference.

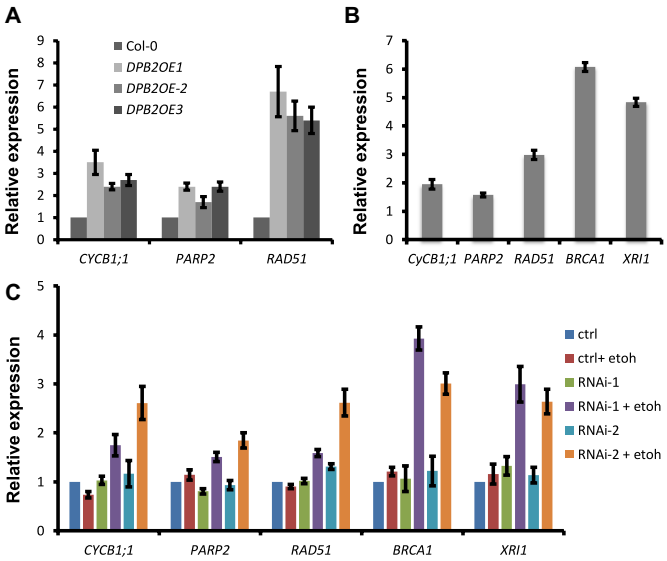

Figure 5. *DPB2OE* plants display symptoms of DNA damage accumulation. (**A**) Transcript levels of DNA damage-induced genes *CYCB1*, *PARP2*, and *RAD51* in *DPB2OE* flowers were measured by quantitative RT-PCR and normalized to PDF2. (**B** and **C**) Transcript levels of DNA damage-induced genes *CYCB1*, *PARP2*, *RAD51, BRCA1* and *XRI-1* in *abo4-1* seedlings (**B**) or DPB2-RNAi seedlings (**C**) were measured by quantitative RT-PCR and normalized to PDF2. For all panels, values are normalized with respect to wild-type (Col-0). In (C), expression was monitored in all genotypes both in absence and in the presence of ethanol. Values are average ± SD from three technical replicates and are representative of two independent experiments.

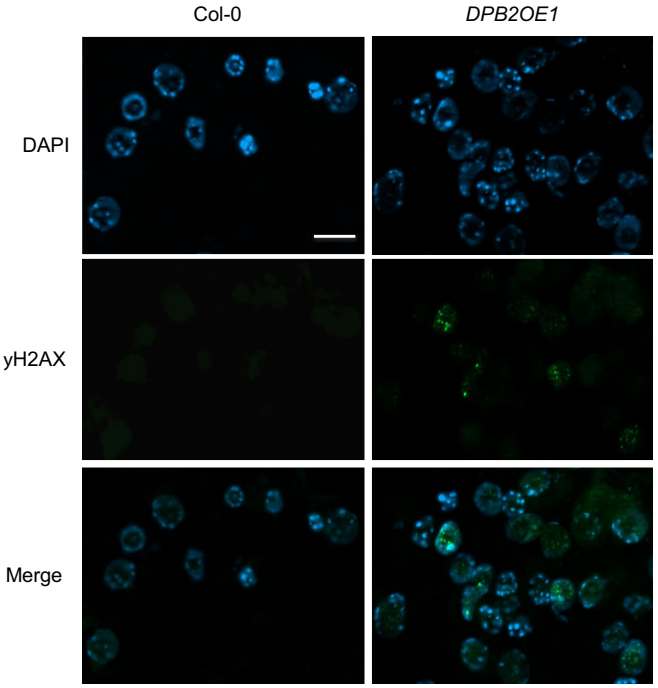

Figure 6. Detection of γ-H2AX immunofluorescence in root tip nuclei. No foci were detected in Col-0 (left panel) plants, while *DPB2OE* nuclei displayed foci (right panel). DNA was stained with DAPI (blue), γ-H2AX foci are colored in Green, and merged images overlay γ-H2AX foci onto nuclei. Bar = 10 μm for all panels.

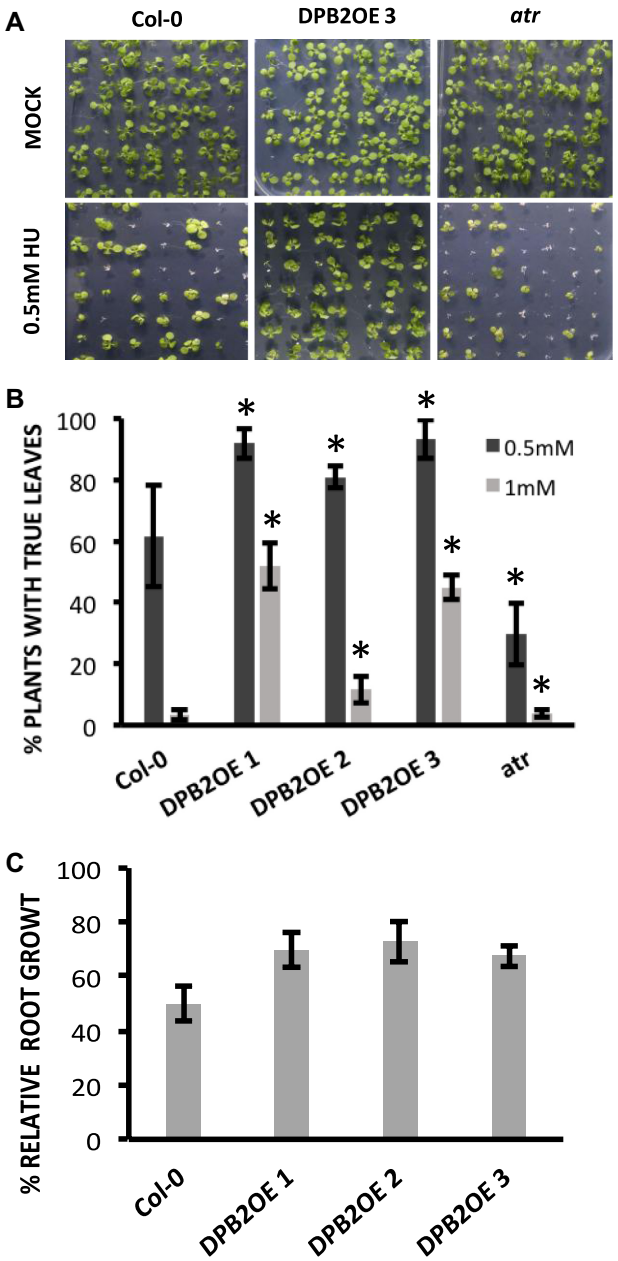

Figure 7. DPB2 over-expression enhances tolerance to replication stress. (**A**) Phenotype of 10-day-old of wild-type (Col-0), *DPB2OE*, and *atr* seedlings germinated with and without HU (0.5mM), (**B**) Relative percentage of plants with true leaves in the presence of 0.5 or 1mM HU, relative to mock-treated populations. Values are mean ± SE of at least three biological replicates with 80–100 seedlings each. (**C**) Quantification of root length of HU-grown seedlings. Four-day-old seedlings were transferred to half-strength MS containing HU (2.0 mM) and root length after was measured after 4 days. Results are expressed as relative growth with respect to the corresponding genotype without treatment. Values are mean ± SE of three biological replicates with 20 seedlings each. For (B) and (C), the asterisks denote significant differences with respect to wild-type plants (Student's *t* test; $P < 0.05$).

sions (44) and zeocin that intercalates DNA and directly cleaves it (45). *DPB2OE* lines were tolerant to all genotoxic stresses tested (Supplementary Figure S9), although the tolerance was more pronounced in the case of UV than upon DSB-inducing treatments. Together our results indicate that at variance with deficiency in the catalytic sub-unit that results in hypersensitivity to all kinds of DNA damage, DPB2 over-expression induces a mild but statistically robust increase in DNA damage tolerance.

Genetic analysis reveals complex interactions of DPB2 function with DDR

The tolerance to different types of DNA damage that trigger replicative stress or DNA breaks, may be due to constitutive activation of ATR, and/or ATM. To investigate the contribution of the DNA damage response to the growth defects caused by DPB2 over-expression, the *DPB2OE* construct was introduced in *atm*, *atr*, and *sog1* mutants. For each background, two transformation batches were analysed and at least 63 plants of each T1 generation were grown in the greenhouse. We were able to identify plants displaying a clear *DPB2OE* phenotype in the T1 generation in all backgrounds (Table 3, Supplementary Figure S10A–C), but the distribution of plants in the different phenotypic categories was significantly different from what was observed in the wild-type in all genotypes (χ^2, P-value < 0.01). *DPB2* over-expression was quantified using qRT-PCR in different lines representative of the different phenotypic groups (Supplementary Figure S10D). Interestingly, plants with similar phenotypes in the Col-0, *atm* or *sog1* background had similar *DPB2* expression levels. By contrast, in the *atr* background, much higher *DPB2* over-expression was required to induce severe and intermediate developmental defects, indicating that ATR activation accounts for some of the phenotypic alterations induced by *DPB2* over-expression. Root growth assays confirmed that plants had been assigned to the proper phenotypic category: root growth inhibition was similar in the severe, intermediate and mild lines of all tested backgrounds (Supplementary Figure S11). Interestingly, viable plants with very severe phenotype could only be obtained in the *sog1*, and *atr* backgrounds (Supplementary Figure S10A and B), but many of these plants died before flowering, and they were obtained at a lower frequency than in the Col-0 background (Table 3). In the *atm* background, we only identified plants with intermediate and mild vegetative phenotype (Supplementary Figure S10C). These results suggest that ATM is required for survival of severe *DPB2OE* lines. However, failure to obtain plants with severe phenotype may also be due to 35S interference that would prevent *DPB2* expression to reach sufficient levels, since the *atm* mutant allele was from the SALK collection (46). To determine whether ATM activity was essential to *DPB2OE* plants survival, we tested the effect of a specific inhibitor of ATM activity (IATM), and found that *DPB2OE* lines are hypersensitive to this drug (Supplementary Figure S12) supporting the notion that ATM activity is required for survival of *DPB2OE* whereas SOG1 and ATR are not. To further analyse the genetic interaction between *SOG1* and *DPB2*, we asked whether the tolerance to DNA damage observed in *DPB2OE* lines required SOG1 activation. To this end, we assessed the sensitivity of *sog1* and *sog1DPB2OE* to HU. As previously demonstrated (47), *sog1* was hypersensitive to HU, and *sog1 DPB2OE* displayed an intermediate phenotype between wild-type and *sog1* mutants (Fig-

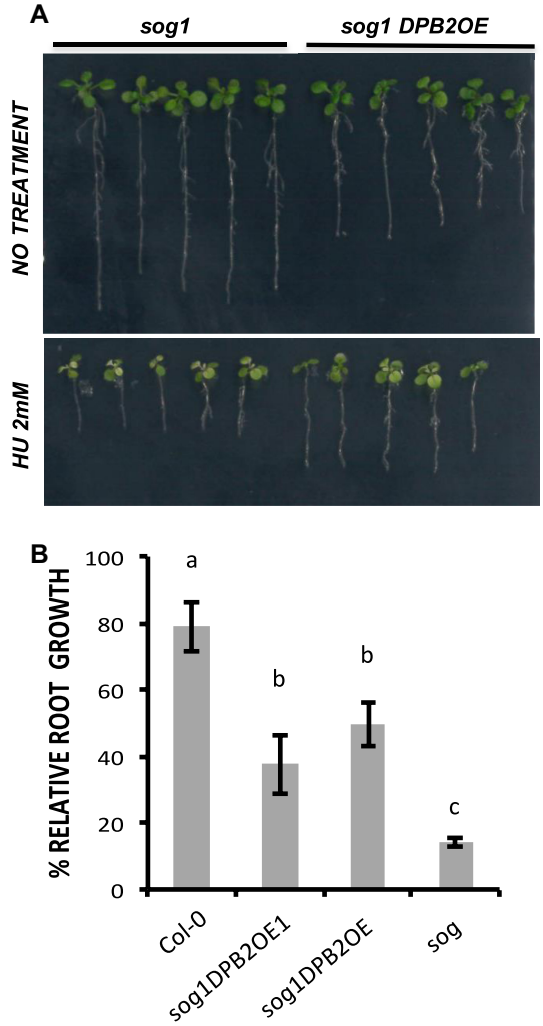

Figure 8. DPB2 over-expression partially rescues HU hypersensitivity in the *sog1* mutant. A, B: Seedlings were germinated and grown on 0.5× MS medium for 4 days and transferred either to 0.5× MS medium or 0.5× MS medium supplemented with 2 mM of HU. (**A**) phenotype of *sog1* and *sog1DPB2OE* seedlings after 8 d with or without treatment; (**B**) relative root growth. Results are shown as relative length with respect of the corresponding genotype without treatment, and values are mean ± SE of three biological replicates with 20 seedlings each. Letters indicate statistically significant differences (Student's *t* test; $P < 0.05$).

ure 8A-B). This additivity of the *sog1* and *DPB2OE* phenotypes suggests that DPB2 and SOG1 control HU sensitivity via independent pathways. This is further corroborated by the observation that some DNA damage response genes were up-regulated in flower buds despite of SOG1 deficiency in *sog1 DPB2OE* lines (Supplementary Figure S13): induction of *XRI-1*, *PAPR2*, *BRCA1* or *SMR5* and *7* was lost or greatly reduced in the *sog1* background. Surprisingly, *WEE1*, *CYCB1;1* and *RAD51* were still up-regulated in the *sog1* mutant, indicating that DPB2 over-accumulation activates a SOG1-independent replicative stress checkpoint. Together, these results indicate that ATR and SOG1 are dispensable to the survival of *DPB2OE* lines, and that their activation only partly accounts for growth retardation observed in *DPB2OE* lines.

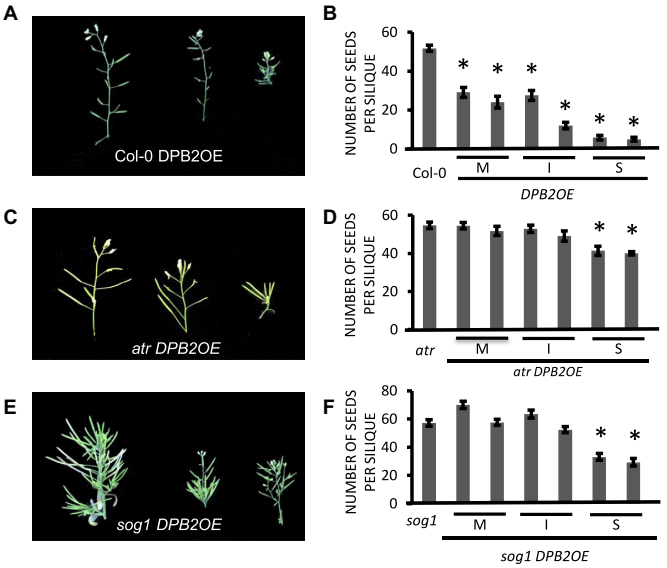

Figure 9. Sterility caused by *DPB2* over-expression largely depends on SOG1 and ATR activity. Panels (**A**), (**C**) and (**E**) show the representative siliques phenotype of *DPB2* over-expressing Col-0, *atr,* and *sog1* lines. (**B**), (**D**) and (**F**) show the average number of seeds produced per silique in independent *DPB2OE* lines displaying mild (M), intermediate (I) and severe (S) phenotypes, corresponding to the phenotypes of *DPB2OE* lines 3, 2 and 1 respectively. Values are mean ± SE ($n = 30$) for each line. For (B), (D) and (E), the asterisks denote significant differences with respect to the background in which *DPB2OE* was introduced (Student t test; $P < 0.05$).

Unexpectedly, inactivation of ATR and SOG1 rescued the fertility of *DPB2OE* lines (Figure 9A–F). This effect was particularly striking in the *sog1* background: we observed that plants with identical *DPB2* mRNA levels were as severely affected as in the Col-0 background with respect to plant size, but the above-described sterility phenotype was completely lost (Figure 9F). The *sog1 DPB2OE* lines were propagated until the T5 generation, and the observed fertility rescue was conserved. Most of obtained seeds germinated although 30–40% died at the seedling stage. This result suggests that the partial sterility of *DPB2OE* plants is dependent of SOG1 protein function. Analysis of meiosis progression in the most severe *sog1 DPB2OE* lines confirmed that DNA fragmentation was largely lost (Supplementary Figure S14), indicating that the meiotic DNA-fragmentation phenotype observed in *DPB2OE* lines is an active process requiring SOG1. Together, our results indicate that DPB2 over-expression activates distinct DDR pathways during the vegetative and reproductive phases.

DISCUSSION

DNA polymerase ϵ plays a key role during DNA replication. Until recently, it was considered as the polymerase responsible for the synthesis of the leading strand, but evidence suggest that its main role may be in the progression of the CMG complex to unwind the replication fork and in the repair of replication errors (5). Here, we have investigated the role of the regulatory sub-unit DPB2 in Arabidopsis using an over-expression strategy to overcome the lethality of DPB2 deficiency (14). DPB2 over-expression impairs the replicative function of the Pol ϵ complex. Indeed, *DPB2OE*

Table 3. Distribution of *DPB2OE* T1 plants in the mild, intermediate and severe phenotypic classes in the wild-type (Col-0) and DDR mutant backgrounds

Line	Mild	Intermediate	Severe	Total
Col-0 *DPB2OE*	40	23	25 (4)	88
	59	26	32 (3)	117
atr DPB2OE	54	18	11 (5)	83
	46	12	7 (3)	65
atm DPB2OE	56	6	1 (1)	63
	74	11	0	85
sog1 DPB2OE	9	35	29 (18)	73
	15	53	24 (14)	92

Transgenic plants were selected on sand watered with glufosinate. For each background, two independent transformations were performed, which corresponds to the two rows. The indicated number of T1 plants was transferred to the green house, and phenotypes were scored. For the 'Severe' category, numbers in brackets indicate the number of plants that died before flowering.

lines displayed the same aphidicolin sensitivity and the same early flowering phenotype as *abo4*/*esd7* mutant lines that are deficient for the catalytic sub-unit (18,19). Because complementation experiments demonstrate that the CFP-DPB2 protein is functional, we can rule out the possibility that the phenotype of DPB2OE lines could be the result of a dominant-negative effect. Additionally, inducible inactivation of DPB2 via RNAi induced similar cell cycle delay and root growth inhibition as DPB2 over-expression. Analysis of the native holoenzyme purified from yeast suggests a 1:1:1:1 stoichiometry for the Pol ϵ sub-units (48); although the complex composition has not been investigated in plants, our results reveal the importance of stoichiometric sub-unit accumulation for complex functionality. In yeast, DPB2 is not required for Pol2A catalytic activity *in vitro*, but it improves its stability (49), and enhances the fidelity of DNA replication (50). Recently, Sengupta *et al.* (7) have shown that DPB2 is required to integrate DNA Pol ϵ into the replisome, and that over-expression of the N-terminus of DPB2 is sufficient to rescue the lethality of *dpb2* null mutants. These lines are capable to produce a replisome lacking Pol ϵ and are viable although they grow extremely poorly (7). Strikingly, over-expression of DPB2 N-terminus has a dominant negative effect, and yeast cells with a replisome lacking Pol2A show delayed S-phase progression, as is the case for *DPB2OE* lines. Our results therefore suggest that plant DPB2 protein functions like its yeast counterpart to link Pol ϵ and the helicase into a functional replisome.

Detailed phenotypic analysis of *DPB2OE* lines revealed dramatic defects both in the mitotic and the meiotic cell cycle. In somatic cells, DPB2 over-expression led to a delay in S-phase progression as reported in Pol2A-deficient mutants (16,18), further supporting the notion that defects caused by DPB2 over-expression are due to impaired Pol ϵ functionality. Interestingly, the observed increase in S-phase length did not fully account for the total increase in cell cycle length. Together with the enhanced expression of the G2/M marker *CYCB1;1*, this result points to constitutive activation of the DDR and subsequent cell cycle checkpoint activation in *DPB2OE* lines, leading to a G2 arrest. Eukaryotic cells respond to DNA replication block or DNA damage by activating checkpoints that delay the onset of mitosis until DNA replication and repair are completed (28). *DPB2OE* lines display several features observed in response to DNA stress including *CYCB1;1* over-expression, enhanced endoreduplication likely reflecting early onset of differentiation, and increased expression of DNA repair genes (28). Similar defects were reported in several mutants deficient for proteins involved in DNA replication such as *caf* (*chromatin assembly factor*), *fas1* (*fasciata*), *pol2a*, *rpa2a (replication protein a)*, (18,51–53), and were hypothesized to result from stalled replication forks during S-phase (18,28). Consistently, we were able to show that *DPB2OE* lines constitutively accumulate DNA damage, as evidenced by the presence of phosphorylated γH2A-X foci in root meristem nuclei, suggesting that altered fork progression in these lines ultimately leads to fork collapse and formation of DSB. Taken together, our results strongly suggest that control of DPB2 accumulation plays a key role at the replication fork to prevent DNA damage from accumulating during replication.

To further explore the role of DPB2 in DNA replication and repair, we tested the sensitivity of *DPB2OE* lines to replication stress and direct DNA damage. By contrast to mutations in replisome sub-units, DPB2 over-expression conferred tolerance to replicative stress induced by hydroxyurea as well as to DNA-damaging agents. The increased tolerance to DNA damage could be due to basal activation of the DNA stress checkpoints and constitutive expression of DNA repair genes, as proposed in the case of CDT1-deficient lines (54), as well as to activation of bypass mechanisms allowing DNA replication to proceed through lesions. This hypothesis correlates with the basal increase in the transcription of DNA repair genes and the presence of phosphorylated form of H2AX histone variant (γH2AX), which plays a key role in the recruitment and accumulation of DNA repair proteins at sites of DSBs (55). Consistently, the line displaying the highest basal accumulation of DSB is not tolerant to zeocin, suggesting that DPB2 over-accumulation confers tolerance to DNA damage up to a certain threshold above which pre-activation of DNA repair pathways is not sufficient for the plant to cope with genotoxic stress. Thus DPB2 over-expression likely triggers the pre-activation of DNA damage response, resulting in less growth inhibition after of DNA damage exposure. Intriguingly, *DPB2OE* lines shared features with the Pol ϵ catalytic subunit mutant (*abo4-1*) in the alterations of cell cycle and DNA repair genes increased transcript levels, suggesting also the pre-activation of DDR in *abo4-1*, however, this mutant is hyper-sensitive to DNA damaging agents such as MMS and UV-C (18). POL2A participates in various DNA repair pathways such as nucleotide excision

repair (NER), base excision repair (BER), break-induced replication (BIR), and homologous recombination (HR) (56,57) in many organisms. Our observation that DPB2 over-expression interferes with DNA replication but not with DNA repair suggests that POL2A functions independently of DPB2 in DNA repair, or that the relative abundance of the two sub-units plays a less prominent role in this pathway. Regarding the observed tolerance to HU, it could either reflect this improved tolerance to various kinds of DNA damage, or the impairment of Pol ϵ-dependent S-phase checkpoint activation. Since our work nevertheless indicates that ATR is activated by DPB2 over-expression, one can postulate that multiple sensing mechanisms cooperate at the fork to signal defects in replication progression to downstream components some possibly mediated by Pol ϵ itself, and others mediated via the formation of single stranded DNA upon uncoupling of the replicative machinery and the helicase complex. Indeed Pol ϵ catalytic subunit is required for the activation of the S-phase checkpoint upon replication defects such as fork stalling, collapse or DNA damage (12,58), and this role has recently been shown to require Pol ϵ association into the replisome (59); hence, impairment of Pol ϵ association to the replisome by DPB2 over-expression may prevent checkpoint activation in these lines.

To further connect DPB2 functions with DDR, we have used genetic approaches. The frequency of lines displaying a severe phenotype in the T1 generation was reduced in both *atm* and *atr* mutants, which may suggest that the two kinases contribute to the survival *DPB2OE* plants. In the case of *atm*, this is supported by the hypersensitivity of *DPB2OE* lines to an inhibitor of ATM and the fact that we could not recover plants with a high DPB2 over-expression or a severe phenotype. By contrast, we observed very high accumulation of *DPB2* mRNA in *atr DPB2OE* lines that did not result in a severe phenotype, indicating that ATR activation is partly responsible for the growth defects in *DPB2OE* lines. It is worth noting that the few plants displaying a severe phenotype had a poor survival rate, suggesting that failure to activate ATR-dependent responses can lead to developmental arrest likely caused by extensive DNA damage. By contrast, plants with intermediate and severe phenotype were obtained at a higher frequency in the *sog1* mutant, and root growth inhibition was slightly more pronounced in the *sog1* than in the Col-0 background for lines with similar levels of *DPB2* accumulation (Supplementary Figure S11), suggesting that SOG1 activation partially alleviates defects induced by DPB2 over-expression. However, the survival rate of severe lines was lower than in the wild-type, indicating that SOG1 also contributes to the viability of these plants. Meristem arrest caused by DPB2 over-expression in the *sog1* background may also account for the bushy appearance of *sog1 DPB2OE* plants, as arrest of the main meristem would favour branching. In addition, the *sog1* mutation restored only partially the sensitivity to HU of *DPB2OE* roots, and some DNA damage response genes were still up-regulated in flower buds despite of SOG1 deficiency. Recently, Hu *et al.* have reported that replication checkpoint activation upon HU treatment relies on two parallel pathways: one involving WEE1 activation via the ATR kinase, and the other involving SOG1 activation via ATR (47) (Figure 10A, black arrows). Our results are consistent with the notion that SOG1 is not the only regulator of this checkpoint. Interestingly, they also show that *CYCB1;1*, that is activated in a SOG1-dependent manner by DNA damage (24), is activated via SOG1-independent pathways by Pol ϵ dysfunction. Together our results suggest that replication stress induced by DPB2 over-accumulation activates the ATR-SOG1 module that is required for sustained growth, possibly via its role in the regulation of DNA repair genes. In parallel, ATR regulates cell cycle progression independently of SOG1, and in the absence of ATR, plants show a less pronounced growth inhibition but lower survival. In addition, ATM appears to be required for survival of *DPB2OE* lines, indicating that DPB2 over-expression also leads to fork collapse and DSB formation, which would activate DDR in an ATR-independent manner. Indeed, proteins from the mitogen-activated protein (MAP) kinase pathway have been shown to play a role in DDR independently of ATR and could thus be activated by Polϵ deficiency (60). Figure 10A summarizes the proposed model for the effect of DPB2 over-expression in vegetative

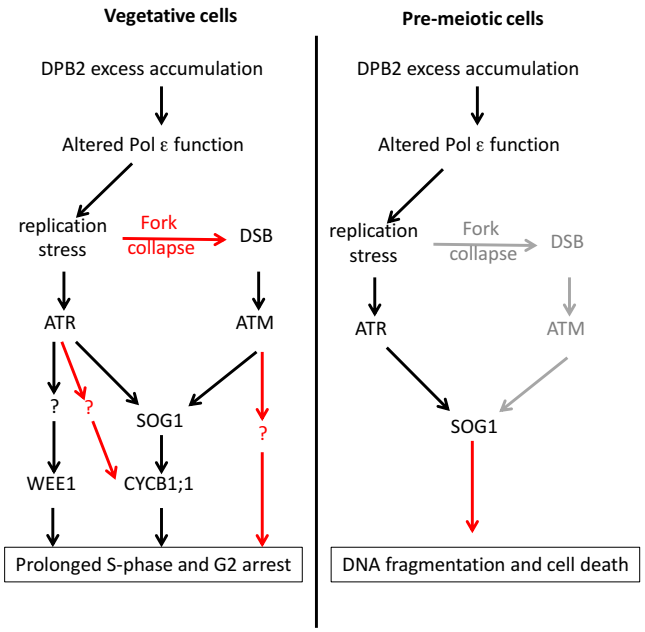

Figure 10. Involvement of DPB2 in DDR regulation in somatic and reproductive cells. (**A**) In vegetative cells, excess DPB2 accumulation alters Pol ϵ function either by excluding Pol2A from the replication fork or by altering the stability of protein complexes at the fork. This leads to fork stalling and replication stress, thereby activating ATR which in turn can delay cell cycle progression by activating WEE1 and CYCB1;1 and possibly other cell cycle regulators. This activation occurs independently of SOG1, even though CYCB1;1 is a known target of this transcription factor. In addition, altered fork progression leads to fork collapse and creation of DSB, which activate ATM. The observation that ATM but not SOG1 is required for survival of *DPB2OE* lines indicates that unknown SOG1-independent pathways are required to regulate cell cycle progression and DNA repair upon fork collapse. (**B**) In pre-meiotic cells, the above-described initial events occur similarly, but in this tissue, SOG1 activation leads to an active process of DNA fragmentation probably associated with cell death. This mechanism may represent a pre-meiotic replication specific checkpoint that would prevent transmission of replication errors through gametogenesis. Arrows in red represent regulatory pathways inferred from this work, whereas black arrows correspond to previously identified mechanisms.

cells; together our results indicate that perturbed Pol ϵ function activates the two main DNA stress response pathways previously described in plants, but also provide evidence for yet unidentified regulatory pathways. Notably, they demonstrate that SOG1-independent pathways can activate both DNA repair genes and cell cycle delay.

In addition to the defects observed in somatic cells, severe *DPB2OE* lines showed DNA fragmentation during meiosis. Similar defects have been reported in various mutants deficient for replisome sub-units such as *CDC45-RNAi* lines, *rpa*, or *abo4-2* (53,61,62). The chromosome fragmentation observed in all these lines could be due to defects during premeiotic DNA replication, which is essential to chromosome cohesion, meiotic recombination and chromosome segregation, but could also reflect a role of the replicative machinery in DSB repair via homologous recombination. Consistently, POL2A is expressed in meiocytes in mouse (63) and in Arabidopsis (62). Furthermore, meiotic defects observed in Arabidopsis POL2A-deficient lines were SPO11-dependent, suggesting that they were due to defects in DNA repair (62). By contrast, disruption of CDC45 or MEI1, like DPB2 over-expression, results in SPO11-independent DNA fragmentation, suggesting that defects occurred during premeiotic replication (61,64). Because DPB2 forms complexes with CDC45 and MEI1 in different steps of replication initiation where the catalytic subunit is not required (65), its over-expression could affect the stability of interactions required for correct DNA replication prior to meiosis, leading to delayed completion of DNA replication or replication errors. Strikingly, although SOG1 is essential to normal meiosis in the *uvh1* background (66), the fertility of *DPB2OE* lines was restored in the *sog1* background, and DNA fragmentation was largely lost. Hence, our results provide evidence for the involvement of SOG1 in an active DNA fragmentation program triggered by replication defects in meiocytes (Figure 10B), consistent with the role of SOG1 in the transcriptional activation of cell death genes (24,67). This hypothesis is further supported by the observation that the survival of *sog1 DPB2OE* T2 seedlings was affected, suggesting that a large proportion of embryos derived from gametes with major genetic anomalies. Interestingly, in mammals, a link exists between the regulation of Pol ϵ activity and p53, the functional homologue of SOG1: MDM2 (Mouse Double Minute 2) can bind the C-terminus of Pol2A and is thought to simultaneously modulate Pol ϵ functions in response to stress and control cell cycle progression by regulating p53 degradation (68), similar mechanisms might be conserved in plants to maintain genome integrity.

Overall, our work provides evidence for the exquisite complexity of DNA damage and replication stress response in plants, and further questions the central role of SOG1 as the central integrator of DNA damage response in plant cells. Additionally, it reveals the tissue specificity of cellular responses, defects in pre-meiotic DNA replication triggering a cell death response that does not occur in vegetative tissues in response to Pol ϵ dysfunction.

DATA DEPOSITION

Microarray data from this article were deposited at Gene Expression Omnibus (http://www.ncbi.nlm.nih.gov/geo/), accession no. GSE71002) and at CATdb (http://urgv.evry.inra.fr/CATdb/; Project: NGS2014_10_Epsilon) according to the 'Minimum Information About a Microarray Experiment' standards.

ACCESSION NUMBERS

Sequence data from this article can be found in the Arabidopsis Genome Initiative or GenBank/EMBL databases under the following accession numbers: *DPB2* (AT5G22110), *SMR5* (AT1G07500), *SMR7* (AT3G27630), *PARP2* (AT2G31320), *KU70* (AT1G16970), *CYCB1-1* (AT4G37490), *XRI1* (AT5G48720), *WEE1* (AT1G02970), *BRCA1* (AT4G21070).

SUPPLEMENTARY DATA

Supplementary Data are available at NAR Online.

ACKNOWLEDGEMENTS

We thank Lieven De Veylder (VIB, Gent) and Patricia Kannouche (IGR, Villejuif), for helpful discussions about this work. The present work has benefited from the core facilities of Imagerie-Gif, (http://www.i2bc.paris-saclay.fr), member of IBiSA (http://www.ibisa.net), supported by the Labex 'Saclay PlantScience' (ANR-11-IDEX-0003-02).

FUNDING

Agence Nationale de la Recherche [ANR 2010 JCJC1207 01]; J.A.P.G. benefited from a doctoral contract of the Paris-Sud University. Funding for oen access charge: Agence Nationale de la Recherche [ANR 2010 JCJC1207 01].
Conflict of interest statement. None declared.

REFERENCES

1. Heyman,J., Kumpf,R.P. and De Veylder,L. (2014) A quiescent path to plant longevity. *Trends Cell Biol.*, **24**, 443–448.
2. Kurth,I. and O'Donnel,M. (2013) New insights into replisome fluidity during chromosome replication. *Trends Biochem Sci.*, **38**, 195–203.
3. Garg,P. and Burgers,P.M.J. (2005) DNA polymerases that propagate the eukaryotic DNA replication fork. *Crit. Rev. Biochem. Mol. Biol.*, **40**, 115–128.
4. Pursell,Z.F., Isoz,I., Lundstrom,E.B., Johansson,E. and Kunkel,T.A. (2007) Yeast DNA polymerase epsilon participates in leading-strand DNA replication. *Science*, **317**, 127–130.
5. Johnson,R.E., Klassen,R., Prakash,L. and Prakash,S. (2015) A major role of DNA polymerase δ in replication of both the leading and lagging DNA strands. *Mol. Cell*, **59**, 1–13.
6. Pursell,Z.F. and Kunkel,T.A. (2008) DNA polymerase epsilon: a polymerase of unusual size (and complexity). *Prog. Nucleic Acids Res. Mol. Biol.*, **82**, 101–145.
7. Sengupta,S., Van Deursen,F., De Piccoli,G. and Labib,K. (2013) Dpb2 Integrates the Leading-Strand DNA Polymerase into the Eukaryotic Replisome. *Curr. Biol.*, **23**, 543–552.
8. Langston,L.D., Zhang,D., Yurieva,O., Georgescu,R.E., Finkelstein,J., Yao,N.Y., Indiani,C. and O'Donnell,M.E. (2014) CMG helicase and DNA polymerase form a functional 15-subunit holoenzyme for eukaryotic leading-strand DNA replication. *Proc. Natl. Acad. Sci. U.S.A.*, **111**, 15390–15395.

9. Navas,T.A., Zhou,Z. and Elledge,S.J. (1995) DNA polymerase epsilon links the DNA replication machinery to the S phase checkpoint. *Cell*, **80**, 29–39.
10. Roseaulin,L.C., Noguchi,C., Martinez,E., Ziegler,M.A., Toda,T. and Noguchi,E. (2013) Coordinated degradation of replisome components ensures genome stability upon replication stress in the absence of the replication fork protection complex. *PLoS Genet.*, **9**, e1003213.
11. Branzei,D. and Foiani,M. (2009) The checkpoint response to replication stress. *DNA Repair (Amst.)*, **8**, 1038–1046.
12. Puddu,F., Piergiovanni,G., Plevani,P. and Muzi-Falconi,M. (2011) Sensing of replication stress and Mec1 activation act through two independent pathways involving the 9-1-1 complex and DNA polymerase ϵ. *PLoS Genet.*, **7**, e1002022.
13. Van Leene,J., Stals,H., Eeckhout,D., Persiau,G., Van De Slijke,E., Van Isterdael,G., De Clercq,A., Bonnet,E., Laukens,K., Remmerie,N. *et al.* (2007) A tandem affinity purification-based technology platform to study the cell cycle interactome in Arabidopsis thaliana. *Mol. Cell. Proteomics*, **6**, 1226–1238.
14. Ronceret,A., Guilleminot,J., Lincker,F., Gadea-Vacas,J., Delorme,V., Bechtold,N., Pelletier,G., Delseny,M., Chaboute,M.E. and Devic,M. (2005) Genetic analysis of two Arabidopsis DNA polymerase epsilon subunits during early embryogenesis. *Plant J.*, **44**, 223–236.
15. Petroni,K., Kumimoto,R.W., Gnesutta,N., Calvenzani,V., Fornari,M., Tonelli,C., Holt,B.F. and Mantovani,R. (2012) The promiscuous life of plant NUCLEAR FACTOR Y transcription factors. *Plant Cell*, **24**, 4777–4792.
16. Jenik,P.D., Jurkuta,R.E. and Barton,M.K. (2005) Interactions between the cell cycle and embryonic patterning in Arabidopsis uncovered by a mutation in DNA polymerase epsilon. *Plant Cell*, **17**, 3362–3377.
17. Sato,H., Mizoi,J., Tanaka,H., Maruyama,K., Qin,F., Osakabe,Y., Morimoto,K., Ohori,T., Kusakabe,K., Nagata,M. *et al.* (2014) Arabidopsis DPB3-1, a DREB2A interactor, specifically enhances heat stress-induced gene expression by forming a heat stress-specific transcriptional complex with NF-Y subunits. *Plant Cell*, **26**, 4954–4973.
18. Yin,H., Zhang,X., Liu,J., Wang,Y., He,J., Yang,T., Hong,X., Yang,Q. and Gong,Z. (2009) Epigenetic regulation, somatic homologous recombination, and abscisic acid signaling are influenced by DNA polymerase epsilon mutation in Arabidopsis. *Plant Cell*, **21**, 386–402.
19. del Olmo,I., Lopez-Gonzalez,L., Martin-Trillo,M.M., Martinez-Zapater,J.M., Pineiro,M. and Jarillo,J.A. (2010) EARLY IN SHORT DAYS 7 (ESD7) encodes the catalytic subunit of DNA polymerase epsilon and is required for flowering repression through a mechanism involving epigenetic gene silencing. *Plant J.*, **61**, 623–636.
20. Del Olmo,I., López,J.A., Vázquez,J., Raynaud,C., Piñeiro,M. and Jarillo,J.A. (2016) Arabidopsis DNA polymerase ε recruits components of Polycomb repressor complex to mediate epigenetic gene silencing. *Nucleic Acids Res.*, doi:10.1093/nar/gkw156.
21. Yoshiyama,K.O., Sakagushi,K. and Kimura,S. (2013) DNA damage response in plants: conserved and variable response compared to animals. *Biology (Basel)*, **2**, 1338–1356.
22. Culligan,K., Tissier,A. and Britt,A. (2004) ATR regulates a G2-phase cell-cycle checkpoint in Arabidopsis thaliana. *Plant Cell*, **16**, 1091–1104.
23. Culligan,K.M., Robertson,C.E., Foreman,J., Doerner,P. and Britt,A.B. (2006) ATR and ATM play both distinct and additive roles in response to ionizing radiation. *Plant J.*, **48**, 947–961.
24. Yoshiyama,K., Conklin,P.A., Huefner,N.D. and Britt,A.B. (2009) Suppressor of gamma response 1 (SOG1) encodes a putative transcription factor governing multiple responses to DNA damage. *Proc. Natl. Acad. Sci. U.S.A.*, **106**, 12843–12848.
25. Adachi,S., Minamisawa,K., Okushima,Y., Inagaki,S., Yoshiyama,K., Kondou,Y., Kaminuma,E., Kawashima,M., Toyoda,T., Matsui,M. *et al.* (2011) Programmed induction of endoreduplication by DNA double-strand breaks in Arabidopsis. *Proc. Natl. Acad. Sci. U.S.A.*, **108**, 10004–10009.
26. De Schutter,K., Joubes,J., Cools,T., Verkest,A., Corellou,F., Babiychuk,E., Van Der Schueren,E., Beeckman,T., Kushnir,S., Inze,D. *et al.* (2007) Arabidopsis WEE1 kinase controls cell cycle arrest in response to activation of the DNA integrity checkpoint. *Plant Cell*, **19**, 211–225.
27. Fulcher,N. and Sablowski,R. (2009) Hypersensitivity to DNA damage in plant stem cell niches. *Proc. Natl. Acad. Sci. U.S.A.*, **106**, 20984–20988.
28. Cools,T. and De Veylder,L. (2009) DNA stress checkpoint control and plant development. *Curr. Opin. Plant Biol.*, **12**, 23–28.
29. Deveaux,Y., Peaucelle,A., Roberts,G.R., Coen,E., Simon,R., Mizukami,Y., Traas,J., Murray,J.A.H., Doonan,J.H. and Laufs,P. (2003) The ethanol switch: a tool for tissue-specific gene induction during plant development. *Plant J.*, **36**, 918–930.
30. Boyes,D.C., Zayed,A.M., Ascenzi,R., McCaskill,A.J., Hoffman,N.E., Davis,K.R. and Görlach,J. (2001) Growth stage-based phenotypic analysis of Arabidopsis: a model for high throughput functional genomics in plants. *Plant Cell*, **13**, 1499–1510.
31. Langmead,B. and Salzberg,S.L. (2012) Fast gapped-read alignment with Bowtie 2. *Nat. Methods*, **9**, 357–359.
32. Lamesch,P., Berardini,T.Z., Li,D., Swarbreck,D., Wilks,C., Sasidharan,R., Muller,R., Dreher,K., Alexander,D.L., Garcia-Hernandez,M. *et al.* (2012) The Arabidopsis Information Resource (TAIR): improved gene annotation and new tools. *Nucleic Acids Res.*, **40**, D1202–D1210.
33. Ross,K.J., Fransz,P. and Jones,G.H. (1996) A light microscopic atlas of meiosis in Arabidopsis thaliana. *Chromosome Res.*, **4**, 507–516.
34. Hayashi,K., Hasegawa,J. and Matsunaga,S. (2013) The boundary of the meristematic and elongation zones in roots: endoreduplication precedes rapid cell expansion. *Sci. Rep.*, **3**, 2723.
35. Hudik,E., Yoshioka,Y., Domenichini,S., Bourge,M., Soubigout-Taconnat,L., Mazubert,C., Yi,D., Bujaldon,S., Hayashi,H., De Veylder,L. *et al.* (2014) Chloroplast dysfunction causes multiple defects in cell cycle progression in the Arabidopsis crumpled leaf mutant. *Plant Physiol.*, **166**, 152–167.
36. Charbonnel,C., Gallego,M.E. and White,C.I. (2010) Xrcc1-dependent and Ku-dependent DNA double-strand break repair kinetics in Arabidopsis plants. *Plant J.*, **64**, 280–290.
37. Ni,D.A., Sozzani,R., Blanchet,S., Domenichini,S., Reuzeau,C., Cella,R., Bergounioux,C. and Raynaud,C. (2009) The Arabidopsis MCM2 gene is essential to embryo development and its over-expression alters root meristem function. *New Phytol.*, **184**, 311–322.
38. Grelon,M., Vezon,D., Gendrot,G. and Pelletier,G. (2001) AtSPO11-1 is necessary for efficient meiotic recombination in plants. *EMBO J.*, **20**, 589–600.
39. Baranovskiy,A.G., Babayeva,N.D., Suwa,Y., Gu,J., Pavlov,Y.I. and Tahirov,T.H. (2014) Structural basis for inhibition of DNA replication by aphidicolin. *Nucleic Acids Res.*, **42**, 14013–14021.
40. Yi,D., Kamei,C.L.A., Cools,T., Vanderauwera,S., Takahashi,N., Okushima,Y., Eekhout,T., Yoshiyama,K.O., Larkin,J., Van den Daele,H. *et al.* (2014) The Arabidopsis thaliana SIAMESE-RELATED cyclin-dependent kinase inhibitors SMR5 and SMR7 control the DNA damage checkpoint in response to reactive oxygen species. *Plant Cell*, **26**, 296–309.
41. Amiard,S., Charbonnel,C., Allain,E., Depeiges,A., White,C.I. and Gallego,M.E. (2010) Distinct roles of the ATR kinase and the Mre11-Rad50-Nbs1 complex in the maintenance of chromosomal stability in Arabidopsis. *Plant Cell*, **22**, 3020–3033.
42. Charbonnel,C., Allain,E., Gallego,M.E. and White,C.I. (2011) Kinetic analysis of DNA double-strand break repair pathways in Arabidopsis. *DNA Repair (Amst.)*, **10**, 611–619.
43. Rosa,M., Von Harder,M., Cigliano,R.A., Schlögelhofer,P. and Mittelsten Scheid,O. (2013) The Arabidopsis SWR1 chromatin-remodeling complex is important for DNA repair, somatic recombination, and meiosis. *Plant Cell*, **25**, 1990–2001.
44. Fu,D., Calvo,J.A. and Samson,L.D. (2012) Balancing repair and tolerance of DNA damage caused by alkylating agents. *Nat. Rev. Cancer*, **12**, 104–120.
45. Lin,F., Ma,X.-S., Wang,Z.-B., Wang,Z.-W., Luo,Y.-B., Huang,L., Jiang,Z.-Z., Hu,M.-W., Schatten,H. and Sun,Q.-Y. (2014) Different fates of oocytes with DNA double-strand breaks in vitro and in vivo. *Cell Cycle*, **13**, 2674–2680.
46. Daxinger,L., Hunter,B., Sheikh,M., Jauvion,V., Gasciolli,V., Vaucheret,H., Matzke,M. and Furner,I. (2008) Unexpected silencing effects from T-DNA tags in Arabidopsis. *Trends Plant Sci.*, **13**, 4–6.
47. Hu,Z., Cools,T., Kalhorzadeh,P., Heyman,J. and De Veylder,L. (2015) Deficiency of the Arabidopsis helicase RTEL1 triggers a

SOG1-dependent replication checkpoint in response to DNA cross-links. *Plant Cell*, **27**, 149–161.
48. Chilkova,O., Jonsson,B.-H. and Johansson,E. (2003) The quaternary structure of DNA polymerase epsilon from Saccharomyces cerevisiae. *J. Biol. Chem.*, **278**, 14082–14086.
49. Li,Y., Asahara,H., Patel,V.S., Zhou,S. and Linn,S. (1997) Purification, cDNA cloning, and gene mapping of the small subunit of human DNA polymerase epsilon. *J. Biol. Chem.*, **272**, 32337–32344.
50. Jaszczur,M., Flis,K., Rudzka,J., Kraszewska,J., Budd,M.E., Polaczek,P., Campbell,J.L., Jonczyk,P. and Fijalkowska,I.J. (2008) Dpb2p, a noncatalytic subunit of DNA polymerase epsilon, contributes to the fidelity of DNA replication in Saccharomyces cerevisiae. *Genetics*, **178**, 633–647.
51. Endo,M., Ishikawa,Y., Osakabe,K., Nakayama,S., Kaya,H., Araki,T., Shibahara,K., Abe,K., Ichikawa,H., Valentine,L. *et al.* (2006) Increased frequency of homologous recombination and T-DNA integration in Arabidopsis CAF-1 mutants. *EMBO J.*, **25**, 5579–5590.
52. Bolaños-Villegas,P., Yang,X., Wang,H.-J., Juan,C.-T., Chuang,M.-H., Makaroff,C.A. and Jauh,G.-Y. (2013) Arabidopsis CHROMOSOME TRANSMISSION FIDELITY 7 (AtCTF7/ECO1) is required for DNA repair, mitosis and meiosis. *Plant J.*, **75**, 927–940.
53. Aklilu,B.B., Soderquist,R.S. and Culligan,K.M. (2014) Genetic analysis of the Replication Protein A large subunit family in Arabidopsis reveals unique and overlapping roles in DNA repair, meiosis and DNA replication. *Nucleic Acids Res.*, **42**, 3104–3118.
54. Domenichini,S., Benhamed,M., De Jaeger,G., Van De Slijke,E., Blanchet,S., Bourge,M., De Veylder,L., Bergounioux,C. and Raynaud,C. (2012) Evidence for a role of Arabidopsis CDT1 proteins in gametophyte development and maintenance of genome integrity. *Plant Cell*, **24**, 2779–2791.
55. Roy,S. (2014) Maintenance of genome stability in plants: repairing DNA double strand breaks and chromatin structure stability. *Front. Plant Sci.*, **5**, 487.
56. Lange,S.S., Takata,K. and Wood,R.D. (2011) DNA polymerases and cancer. *Nat. Rev. Cancer*, **11**, 96–110.
57. Henninger,E.E. and Pursell,Z.F. (2014) DNA polymerase ϵ and its roles in genome stability. *IUBMB Life*, **66**, 339–351.
58. Feng,W. and D'Urso,G. (2001) Schizosaccharomyces pombe cells lacking the amino-terminal catalytic domains of DNA polymerase epsilon are viable but require the DNA damage checkpoint control. *Mol. Cell. Biol.*, **21**, 4495–4504.
59. García-Rodríguez,L.J., De Piccoli,G., Marchesi,V., Jones,R.C., Edmondson,R.D. and Labib,K. (2015) A conserved Polε binding module in Ctf18-RFC is required for S-phase checkpoint activation downstream of Mec1. *Nucleic Acids Res.*, **43**, 8830–8838.
60. González Besteiro,M.A. and Ulm,R. (2013) ATR and MKP1 play distinct roles in response to UV-B stress in Arabidopsis. *Plant J.*, **73**, 1034–1043.
61. Stevens,R., Grelon,M., Vezon,D., Oh,J., Meyer,P., Perennes,C., Domenichini,S. and Bergounioux,C. (2004) A CDC45 homolog in Arabidopsis is essential for meiosis, as shown by RNA interference-induced gene silencing. *Plant Cell*, **16**, 99–113.
62. Huang,J., Cheng,Z., Wang,C., Hong,Y., Su,H., Wang,J., Copenhaver,G.P., Ma,H. and Wang,Y. (2015) Formation of interference-sensitive meiotic cross-overs requires sufficient DNA leading-strand elongation. *Proc. Natl. Acad. Sci. U.S.A.*, **112**, 12534–12539.
63. Kamel,D., Mackey,Z.B., Sjöblom,T., Walter,C.A., McCarrey,J.R., Uitto,L., Palosaari,H., Lähdetie,J., Tomkinson,A.E. and Syväoja,J.E. (1997) Role of deoxyribonucleic acid polymerase epsilon in spermatogenesis in mice. *Biol. Reprod.*, **57**, 1367–1374.
64. Grelon,M., Gendrot,G., Vezon,D. and Pelletier,G. (2003) The Arabidopsis MEI1 gene encodes a protein with five BRCT domains that is involved in meiosis-specific DNA repair events independent of SPO11-induced DSBs. *Plant J.*, **35**, 465–475.
65. Handa,T., Kanke,M., Takahashi,T.S., Nakagawa,T. and Masukata,H. (2012) DNA polymerization-independent functions of DNA polymerase epsilon in assembly and progression of the replisome in fission yeast. *Mol. Biol. Cell*, **23**, 3240–3253.
66. Preuss,S.B. and Britt,A.B. (2003) A DNA-damage-induced cell cycle checkpoint in Arabidopsis. *Genetics*, **164**, 323–334.
67. Yoshiyama,K.O., Kobayashi,J., Ogita,N., Ueda,M., Kimura,S., Maki,H. and Umeda,M. (2013) ATM-mediated phosphorylation of SOG1 is essential for the DNA damage response in Arabidopsis. *EMBO Rep.*, **14**, 817–822.
68. Vlatkovic,N., Guerrera,S., Li,Y., Linn,S., Haines,D.S. and Boyd,M.T. (2000) MDM2 interacts with the C-terminus of the catalytic subunit of DNA polymerase epsilon. *Nucleic Acids Res.*, **28**, 3581–3586.